The barrier transmission problem treated by the amplitude-phase method and expressed in terms of an invariant of the Ermakov–Lewis type

2005 J. Phys. A: Math. Gen. 38 235

(http://iopscience.iop.org/0305-4470/38/1/017)

INSTITUTE OF PHYSICS PUBLISHING JOURNAL OF PHYSICS A: MATHEMATICAL AND GENERAL

J. Phys. A: Math. Gen. **38** (2005) 235–243 doi:10.1088/0305-4470/38/1/017

The barrier transmission problem treated by the amplitude-phase method and expressed in terms of an invariant of the Ermakov–Lewis type

Karl-Erik Thylwe

Department of Mechanics, Royal Institute of Technology, S-100 44 Stockholm, Sweden

E-mail: ket@mech.kth.se

Received 6 April 2004, in final form 15 October 2004
Published 8 December 2004
Online at stacks.iop.org/JPhysA/38/235

Abstract

Transmission and reflection of a quantal particle by a single-hump potential barrier are analysed by means of an amplitude-phase decomposition of the wavefunction on both sides of the barrier. The amplitude-phase analysis of the wavefunction provides a particular invariant of the Ermakov–Lewis type, which originates in the matching process. The transmission and reflection coefficients turn out to be simple functions of this invariant. Numerical calculations of the invariant for an Eckart–Epstein potential barrier provide very accurate results.

PACS numbers: 02.30.Hq, 02.60.Lj, 03.65.Ca, 03.65.Nk, 03.65.Sq, 03.65.Xp, 52.20.Hv

1. Introduction

Ermakov systems are defined by two intimately connected classes of second-order ordinary differential equations [1–3]; see the appendix. Such nonlinear equations possess an invariant that is a generalization of the well-known Ermakov–Lewis invariant [1, 4–10]. A particular Ermakov system is defined by the equations in the amplitude-phase method [11–15]; see also Pinney [16]. The purpose of the present paper is to demonstrate, by using the amplitude-phase method, that the barrier transmission and reflection coefficients can be expressed in terms of an invariant of the Ermakov–Lewis type. In contrast to the original Ermakov–Lewis invariant, that invariant involves two particular solutions of the nonlinear Milne equation [11]. The calculation of the invariant is found to be accurate and time efficient.

The well-known Ermakov–Lewis invariant [1, 4] plays a formal role in dynamical algebra methods [17] and canonical transformations [18]. There seem to be few applications in wave mechanics (see however [19]), where this invariant enters explicitly as an essential part in the solution of a physical problem.

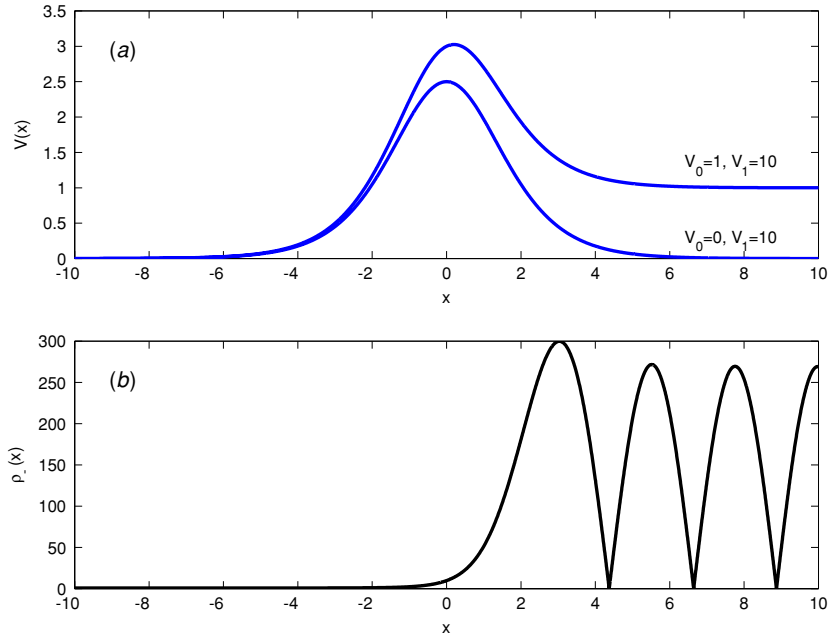

Figure 1. (*a*) Illustration of the Eckart–Epstein potential barrier $V(x)$ in equation (23) for the two sets of parameters $(V_0, V_1) = (0, 10)$ and $(V_0, V_1) = (1, 10)$. For $V_0 = 0$ the barrier is symmetric. (*b*) Behaviour of the Milne solution $\rho_L(x)$, defined by the boundary condition (9*a*). The parameters are $V_0 = 0$, $V_1 = 10$ and $E = 1$. The continuation of $\rho_L(x)$ to the right of the barrier is never used numerically.

The amplitude-phase method used in the present work differs from Milne's original approach, where the solution of the time-independent Schrödinger equation is analysed in terms of a *single* Milne solution (sometimes called the amplitude function). The analysis in the present work uses two Milne solutions. Both solutions satisfy the nonlinear Milne equation but with different boundary conditions.

The ideal situation for an amplitude-phase analysis of the Schrödinger equation would be to use only one non-oscillatory amplitude function, which is the case for the energy quantization problem for a single potential well and simple types of Siegert states [2, 20], and for the phase shift problem of a repulsive scattering potential [14, 21]. However, in other problems, like the calculation of Regge poles [22], resonances [23] and energy quantization in multi-well potentials [2, 24–26], there is no single Milne solution that is non-oscillatory in the entire physical region of space. For example, in the present particular case, the barrier transmission problem, there is one Milne solution that is non-oscillatory to the left of the barrier but becomes strongly oscillating to the right of the barrier; see figure 1. Consequently, the corresponding amplitude-phase decomposition is not in practice useful to the right of the barrier. There is another Milne solution that is non-oscillatory to the right of the barrier, and which develops oscillations to the left of it. The latter solution is the ideal one for analysing the Schrödinger solutions to the right of and in the right part of the barrier. Two Milne solutions are thus needed to cover the whole space with well-behaved amplitude-phase solutions to the Schrödinger equation.

The present paper considers an invariant defined by the two particular Milne solutions discussed above. Both solutions are integrated from their asymptotic boundary conditions

at $-\infty$ and $+\infty$, respectively, to a matching point inside the barrier, where the invariant is calculated. It is found that a point close to the top of the barrier is preferable, since the Milne solutions have similar magnitudes there. In contrast to phase integral and semiclassical approximations, the method does not use the complex plane with its transition points and Stokes and anti-Stokes lines.

The paper is organized as follows: section 2 introduces the Schrödinger equation for the barrier transmission problem and the associated Milne equation. Section 3 explains the matching of two pairs of particular Schrödinger solutions defined by the 'left' Milne solution and by the 'right' Milne solution, respectively. This matching is used in section 4 to obtain explicit expressions for the transmission and reflection coefficients. Comparison of numerical and exact analytic results for the Eckart–Epstein potential barrier is presented in section 5, and a discussion is found in section 6. Invariants of the Ermakov–Lewis type are briefly presented in the appendix.

2. Basic equations

This section summarizes the basic equations needed in the derivation of amplitude-phase formulae for transmission and reflection coefficients.

2.1. Schrödinger equation

The time-independent Schrödinger equation for a quantal particle of mass m and energy E is given by the second-order ordinary differential equation

$$\frac{\mathrm{d}^2\Psi}{\mathrm{d}x^2} + R(x)\Psi = 0, \tag{1}$$

with

$$R(x) = \frac{2m}{\hbar^2}[E - V(x)]. \tag{2}$$

The potential $V(x)$ is assumed to approach constant values as $x \to \pm\infty$, i.e.

$$V(-\infty) = V_L, \tag{3a}$$

$$V(+\infty) = V_R. \tag{3b}$$

The boundary conditions for the wavefunction Ψ can be written as

$$\Psi \sim t\frac{1}{\sqrt{\kappa_L}}\exp(-\mathrm{i}\kappa_L x), \qquad x \to -\infty, \tag{4a}$$

$$\Psi \sim \frac{1}{\sqrt{\kappa_R}}\exp(-\mathrm{i}\kappa_R x) + r\frac{1}{\sqrt{\kappa_R}}\exp(\mathrm{i}\kappa_R x), \qquad x \to +\infty, \tag{4b}$$

where t and r are the transmission and reflection amplitudes, respectively, and

$$\kappa_L = \sqrt{\frac{2m}{\hbar^2}(E - V_L)}, \tag{5a}$$

$$\kappa_R = \sqrt{\frac{2m}{\hbar^2}(E - V_R)}. \tag{5b}$$

The aim is to obtain exact expressions for the transmission and reflection coefficients:

$$T = |t|^2, \tag{6a}$$

$$R = |r|^2. \tag{6b}$$

2.2. Milne equation

The amplitude-phase ansatz consists of

$$\Psi^{(\pm)}(x) = \rho(x)\exp(\pm \mathrm{i}\phi(x)), \tag{7a}$$

$$\frac{\mathrm{d}\phi(x)}{\mathrm{d}x} = \frac{1}{\rho^2(x)}, \tag{7b}$$

where the relation (7*b*) is obtained from the requirement that the Wronskian determinant of the two solutions (7*a*) is constant. Inserting (7*a*) into the Schrödinger equation (1), one obtains the nonlinear Milne equation

$$\frac{\mathrm{d}^2\rho}{\mathrm{d}x^2} + R(x)\rho = \rho^{-3}. \tag{8}$$

Two particular solutions, $\rho_L(x)$ and $\rho_R(x)$, of (8) are of interest in the present investigation. They are defined by being asymptotically constant at $-\infty$ and $+\infty$. They are thus specified by the boundary conditions

$$\rho_L(-\infty) = \kappa_L^{-1/2}, \tag{9a}$$

$$\rho_R(+\infty) = \kappa_R^{-1/2}. \tag{9b}$$

Each one of these Milne solutions defines a pair of independent solutions for the Schrödinger equation:

$$\Psi_L^{(\pm)}(x_0, x) = \rho_L(x)\exp(\pm \mathrm{i}\phi_L(x_0, x)), \qquad \phi_L(x_0, x) = \int_{x_0}^{x} \frac{\mathrm{d}x'}{\rho_L^2(x')}, \tag{10a}$$

$$\Psi_R^{(\pm)}(x_0, x) = \rho_R(x)\exp(\pm \mathrm{i}\phi_R(x_0, x)), \qquad \phi_R(x_0, x) = \int_{x_0}^{x} \frac{\mathrm{d}x'}{\rho_R^2(x')}, \tag{10b}$$

where x_0 is an arbitrary reference point. The same point x_0 will be used later on as matching point to find the relation between $\Psi_L^{(\pm)}(x_0, x)$ and $\Psi_R^{(\pm)}(x_0, x)$.

Note that the phases $\phi_L(x_0, x)$ and $\phi_R(x_0, x)$ in (10*a*) and (10*b*), respectively, which may have to be computed in a general problem but not here, require that the Milne functions have been determined from the boundary conditions (9*a*) and (9*b*).

3. Matching of the solutions of the Schrödinger equation

The present section describes how the two pairs of particular Schrödinger solutions are matched at the point x_0.

In matrix notation, the solutions $\left(\Psi_L^{(+)}(x_0, x), \Psi_L^{(-)}(x_0, x)\right)$ and their derivatives can be expressed in terms of $\Psi_R^{(+)}(x_0, x)$ and $\Psi_R^{(-)}(x_0, x)$ and their derivatives according to

$$\begin{pmatrix} \Psi_L^{(+)}(x_0, x) & \Psi_L^{(-)}(x_0, x) \\ \Psi_L'^{(+)}(x_0, x) & \Psi_L'^{(-)}(x_0, x) \end{pmatrix} = \begin{pmatrix} \Psi_R^{(+)}(x_0, x) & \Psi_R^{(-)}(x_0, x) \\ \Psi_R'^{(+)}(x_0, x) & \Psi_R'^{(-)}(x_0, x) \end{pmatrix} \begin{pmatrix} C_{11} & C_{12} \\ C_{21} & C_{22} \end{pmatrix}, \tag{11}$$

where C_{ij} are the elements of a constant matrix $\mathbf{C}$. This matrix is determined from (11) along with (10*b*) and (10*a*) at the matching point x_0. One obtains

$$\mathbf{C} = \begin{pmatrix} \frac{1}{2}(-\mathrm{i}\mathcal{P} + \mathcal{Q} + \mathcal{Q}^{-1}) & \frac{1}{2}(-\mathrm{i}\mathcal{P} + \mathcal{Q} - \mathcal{Q}^{-1}) \\ \frac{1}{2}(\mathrm{i}\mathcal{P} + \mathcal{Q} - \mathcal{Q}^{-1}) & \frac{1}{2}(\mathrm{i}\mathcal{P} + \mathcal{Q} + \mathcal{Q}^{-1}) \end{pmatrix}, \tag{12}$$

where

$$\mathcal{Q} = \frac{\rho_L(x_0)}{\rho_R(x_0)}, \tag{13a}$$

$$\mathcal{P} = \rho_L'(x_0)\rho_R(x_0) - \rho_R'(x_0)\rho_L(x_0). \tag{13b}$$

For real potentials $\mathcal{Q}$ and $\mathcal{P}$ are real.

4. Transmission and reflection coefficients

In the present section, the wavefunction Ψ satisfying the boundary conditions (4*a*) and (4*b*) is constructed from the particular amplitude-phase solutions discussed in section 2.2. To the left of the barrier the solution $\Psi_L^{(-)}(x_0, x)$ can be written as

$$\Psi_L^{(-)}(x_0, x) \sim \rho_L(x)\,\mathrm{e}^{-\mathrm{i}\kappa_L x}\,\mathrm{e}^{\mathrm{i}\delta_L}, \qquad \text{as} \quad x \to -\infty, \tag{14}$$

where

$$\rho_L(-\infty) = \frac{1}{\sqrt{\kappa_L}}, \tag{15a}$$

$$\delta_L = -\lim_{x\to-\infty}(\phi_L(x_0, x) - \kappa_L x). \tag{15b}$$

The solution $\Psi_L^{(-)}(x_0, x)$ is obviously proportional to the physical solution Ψ to the left of the barrier, and $\Psi_L^{(+)}(x_0, x)$ is thus not needed in this particular problem. With the use of (11), one obtains

$$\Psi_L^{(-)}(x_0, x) = C_{12}\Psi_R^{(+)}(x_0, x) + C_{22}\Psi_R^{(-)}(x_0, x), \tag{16}$$

where according to (4*b*) and (10*b*)

$$\Psi_R^{(\pm)}(x_0, x) \sim \rho_R(x)\,\mathrm{e}^{\pm\mathrm{i}(\kappa_R x + \delta_R)}, \qquad \text{as} \quad x \to +\infty, \tag{17}$$

with

$$\rho_R(+\infty) = \frac{1}{\sqrt{\kappa_R}}, \tag{18a}$$

$$\delta_R = \lim_{x\to+\infty}(\phi_R(x_0, x) - \kappa_R x). \tag{18b}$$

The particular solution $\Psi_L^{(-)}(x_0, x)$ satisfies the boundary condition (14) and, according to (16), (17) and (18*a*), the condition

$$\Psi_L^{(-)}(x_0, x) \sim \frac{C_{12}}{\sqrt{\kappa_R}}\,\mathrm{e}^{\mathrm{i}(\kappa_R x + \delta_R)} + \frac{C_{22}}{\sqrt{\kappa_R}}\,\mathrm{e}^{-\mathrm{i}(\kappa_R x + \delta_R)}, \qquad x \to +\infty. \tag{19}$$

Normalizing (19) according to (4*b*), one finds for the transmission and reflection amplitudes (4*a*) and (4*b*) the formulae

$$t = \mathrm{e}^{\mathrm{i}(\delta_R + \delta_L)}\frac{1}{C_{22}}, \tag{20a}$$

$$r = \mathrm{e}^{2\mathrm{i}\delta_R}\frac{C_{12}}{C_{22}}. \tag{20b}$$

Since the phases δ_L and δ_R in (20*a*) and (20*b*) are real, one finds by means of (12) that the transmission and reflection coefficients defined in (6*a*) and (6*b*) become

$$T = \frac{1}{C_{22}C_{22}^*} = \frac{4}{\mathcal{P}^2 + (\mathcal{Q} + \mathcal{Q}^{-1})^2} = \frac{2}{\mathcal{M}+1}, \tag{21a}$$

$$R = \frac{C_{12}C_{12}^*}{C_{22}C_{22}^*} = \frac{\mathcal{P}^2 + (\mathcal{Q} - \mathcal{Q}^{-1})^2}{\mathcal{P}^2 + (\mathcal{Q} + \mathcal{Q}^{-1})^2} = \frac{\mathcal{M}-1}{\mathcal{M}+1}, \tag{21b}$$

where

$$\mathcal{M} = \tfrac{1}{2}(\mathcal{P}^2 + \mathcal{Q}^2 + \mathcal{Q}^{-2}). \tag{22}$$

The above analysis shows that two particular Milne solutions ρ_L and ρ_R specified by the boundary conditions (9*a*) and (9*b*), respectively, determine an Ermakov–Milne invariant $\mathcal{M}$ (see the appendix), which in turn determines the transmission and reflection coefficients T and R in (21*a*) and (21*b*). Note that the derivations rely only on the amplitude-phase method and that the invariant $\mathcal{M}$ enters in the interpretation of the results.

5. Numerical application

The exact formulae (21*a*) and (21*b*) for the transmission and reflection coefficients, respectively, are expressed in terms of $\mathcal{M}$, which require numerical computations of $\rho_L(x_0)$, $\rho_L'(x_0)$, $\rho_R(x_0)$ and $\rho_R'(x_0)$. To find the accuracy of a standard numerical Runge–Kutta routine (MatLab-rk45), an Eckart–Epstein potential is used for which the Schrödinger equation has exact analytic solutions.

The Eckart–Epstein potential barrier [27–29] with parameters V_0 and V_1 is given by

$$V(x) = V_0\frac{\mathrm{e}^x}{1+\mathrm{e}^x} + V_1\frac{\mathrm{e}^x}{(1+\mathrm{e}^x)^2}, \tag{23}$$

which describes an asymmetric barrier with

$$V(-\infty) = 0, \tag{24a}$$

$$V(+\infty) = V_0. \tag{24b}$$

An exact expression for the reflection coefficient $R = 1 - T$ is derived by Eckart [27]; see also Karlsson [29]. These formulae are used for obtaining the 'exact' reference results denoted by T_{exact} in table 1.

5.1. Direct integration of the Milne equation

The numerical calculations of the Milne solutions needed for T and R in (21*a*) and (21*b*), respectively, are performed with x_0 chosen near the centre position of the barrier. In this way both ρ_L and ρ_R become nonoscillating functions of x as they are integrated numerically from $-\infty$ and $+\infty$, respectively.

Table 1 shows the calculated transmission coefficient T for the Eckart–Epstein barrier with $V_0 = 1.922$ and $V_1 = 11.2$ and a sequence of energies E covering a table in [29]. The units in Milne equation are such that $m/\hbar^2 = 1$. From table 1, it is seen that the direct integration of the Milne equation provides results with relative errors that are consistent with the chosen tolerance in the numerical routine.

Table 1. Calculated values of the transmission coefficient T for the non-symmetric Eckart barrier with $V_0 = 1.922$ and $V_1 = 11.2$, which corresponds to an asymmetric barrier with $V_{\max} = 3.843$. The numerical integrations (with a tolerance of 3×10^{-14}) were initiated at $x = \pm 35$ and the matching was made at an approximate value of the barrier maximum. The relative error of the transmission coefficient has been calculated by means of an exact analytic expression for the transmission coefficient T_{exact} [27]. Throughout this table there are about 13 significant digits in the results.

E	T	$\lvert(T - T_{\text{exact}})/T_{\text{exact}}\rvert$
2	$4.894\,253\,223\,723\,29 \times 10^{-7}$	4×10^{-13}
2.5	$1.559\,372\,292\,527\,55 \times 10^{-4}$	3×10^{-13}
3	0.007 001 207 939 73	3×10^{-13}
3.5	0.143 669 573 206 66	4×10^{-13}
4	0.732 932 800 620 18	7×10^{-14}
4.5	0.971 958 485 460 71	8×10^{-14}
5	0.997 233 823 458 27	2×10^{-15}
5.5	0.999 689 147 168 65	2×10^{-15}
6	0.999 960 473 939 06	5×10^{-15}
10	0.999 999 999 953 11	1×10^{-16}

5.2. Improved numerical integration

Sidky and Ben-Itzhak [23] suggest an improvement compared with the direct integration of Milne's equation in cases where classically forbidden regions become important, as in tunnelling and resonance situations. The Milne solution ρ behaves exponentially in a classically forbidden region and thus an ansatz

$$\rho = \exp(\gamma) \tag{25}$$

is inserted into the Milne equation (8), which becomes

$$\frac{\mathrm{d}^2\gamma}{\mathrm{d}x^2} + \left(\frac{\mathrm{d}\gamma}{\mathrm{d}x}\right)^2 + R(x) = \exp(-4\gamma). \tag{26}$$

This equation replaces Milne's equation, both in the classically allowed and the classically forbidden regions. The phase relation (7*b*), i.e. $\mathrm{d}\phi/\mathrm{d}x = \rho^{-2}$, is due to the substitution (25) replaced by

$$\frac{\mathrm{d}\phi}{\mathrm{d}x} = \exp(-2\gamma). \tag{27}$$

Equation (26) can be used instead of Milne's equation to calculate $\mathcal{M}$. The invariant $\mathcal{M}$ is determined by $\rho_L(x_0) = \exp(\gamma_L(x_0))$ and $\rho_R(x_0) = \exp(\gamma_R(x_0))$ and their derivatives evaluated at the matching point x_0. To obtain these Milne solution values from (26) one calculates solutions γ_L and γ_L satisfying the boundary conditions

$$\gamma_L(x) \to \ln\left(\kappa_L^{-1/2}\right), \qquad \text{as} \quad x \to -\infty, \tag{28a}$$

$$\gamma_R(x) \to \ln\left(\kappa_R^{-1/2}\right), \qquad \text{as} \quad x \to +\infty. \tag{28b}$$

In the present work, this improved numerical method has been tested against the direct integration of the Milne equation. For thick barriers and energies far below the barrier top, the improved calculations often give one further significant digit, but not consistently, given a tolerance of 3×10^{-14}. The main improvement is the reduction in computer time by a factor of approximately 1/3. To see this difference one needs to have situations like for

example the symmetric Eckart–Epstein potential with $V_0 = 0$ and $V_1 = 1000$. Note that the transmission coefficient for $V_0 = 0$, $V_1 = 1000$ and $E = 0.1$ is accurately calculated as $T \approx 2.579\,957\,065\,837 \times 10^{-120}$ with the improved method.

6. Discussion

This investigation shows that the transmission and reflection coefficients for real one-dimensional barriers are simply expressed in terms of an invariant of the Ermakov–Lewis type. The fact that the amplitude-phase method deals with two equations that define an Ermakov system is theoretically interesting, but so far it is mainly unexplored; see however a recent article [19]. It may open up new ideas to improve the amplitude-phase analysis of the time-independent Schrödinger solutions. In recent work Matzkin [30] discusses such an improvement of the amplitude-phase method for bound states in the context of Ermakov systems and the original Ermakov–Lewis invariant.

Ermakov systems have, besides the original Ermakov–Lewis invariant and the present Ermakov–Milne invariant, several other invariants that are recently discussed in the context of the amplitude-phase method (see [19]). In this work the Ermakov–Milne invariant is, apart from its theoretical interest, easily calculated from two particular, non-oscillating solutions of the Milne equation, and the transmission and reflection coefficients obtained are very accurate for single-hump potentials. In extreme cases of thick barriers the computations can be improved as described in section 5.

Acknowledgments

The author is indebted to Professor P O Fröman who has read the manuscript and suggested valuable improvements in the presentation.

Appendix. Ermakov system

A particular Ermakov system may be defined as two coupled, nonlinear differential equations of the form (see [7, 30] and references therein)

$$y'' + R(x)y = y^{-3} f(z/y), \tag{A.1}$$

$$z'' + R(x)z = z^{-3} g(z/y), \tag{A.2}$$

where f and g are functions of their arguments. The invariant for this Ermakov system is given by

$$\mathcal{I} = \frac{1}{2}(z'y - zy')^2 + \int^{z/y} (uf(u) - u^{-3}g(u))\,\mathrm{d}u. \tag{A.3}$$

For the case $f = g = 0$ the invariant $\mathcal{I}$ reduces to a squared Wronskian of two Schrödinger solutions. The original Emakov–Lewis invariant corresponds to putting $f = 0$ and $g = 1$ in (A.1) and (A.2), respectively [1, 2, 4], yielding

$$\mathcal{L} = \frac{1}{2}\left((z'y - zy')^2 + \left(\frac{y}{z}\right)^2\right), \tag{A.4}$$

where y and z are any two solutions of (1) and (8), respectively. Another invariant results from the choice $f = g = 1$, for which (A.1) and (A.2) become two Milne equations [5–7, 10]:

$$\mathcal{M} = \frac{1}{2}\left((z'y - zy')^2 + \left(\frac{y}{z}\right)^2 + \left(\frac{z}{y}\right)^2\right). \tag{A.5}$$

This invariant will be referred to as the Ermakov–Milne invariant. In the present paper, the Ermakov–Milne invariant $\mathcal{M}$ refers to the two particular Milne solutions $z = \rho_L(x)$ and $y = \rho_R(x)$ specified by (9*a*) and (9*b*), respectively.

References

[1] Ermakov V P 1880 *Univ. Izv. Kiev Serie III* **9** 1
[2] Korsch H J and Laurent H 1981 *J. Phys. B: At. Mol. Phys.* **14** 4213
[3] Matzkin A 2001 *J. Phys. A: Math. Gen.* **34** 7833
[4] Lewis H R 1967 *Phys. Rev. Lett.* **18** 510
Lewis H R 1967 *Phys. Rev. Lett.* **18** 636 (erratum)
Lewis H R 1968 *J. Math. Phys.* **9** 1976
Lewis H R and Riesenfeldt W B 1969 *J. Math. Phys.* **10** 1458
Lewis H R and Leach P G L 1982 *J. Math. Phys.* **23** 2371
[5] Lutzky M 1978 *Phys. Lett* A **68** 3
[6] Ray J R and Reid J L 1979 *Phys. Lett.* A **71** 317
Ray J R and Reid J L 1979 *J. Math. Phys.* **20** 2054
[7] Athorne C 1992 *J. Diff. Eqns.* **100** 82
Govindert K S, Athorn C and Leach P G L 1993 *J. Phys. A: Math. Gen.* **26** 4035
[8] George T F, Yeon K-H, Um C-I and Shin S-M 1998 *Phys. Rev.* A **58** 1574
George T F, Yeon K-H, Um C-I and Shin S-M 2000 *Phys. Rev.* A **61** 026103
[9] Haas F 2002 *J. Phys. A: Math. Gen.* **35** 2925
[10] Thylwe K-E 2002 *J. Phys. A: Math. Gen.* **35** 4359
[11] Milne W E 1930 *Phys. Rev.* **35** 863
[12] Wilson H A 1930 *Phys. Rev.* **35** 948
[13] Young H A 1931 *Phys. Rev.* **38** 1612
Young H A 1932 *Phys. Rev.* **39** 455
[14] Wheeler J A 1937 *Phys. Rev.* **52** 1123
[15] Newman W I and Thorson W R 1972 *Can. J. Phys.* **50** 2997
Newman W I and Thorson W R 1972 *Phys. Rev. Lett.* **29** 1350
[16] Pinney E 1950 *Proc. Am. Math. Soc.* **1** 681
[17] Kaushal R S and Korsch H J 1981 *J. Math. Phys.* **22** 1904
[18] Thylwe K-E and Dankowicz H 1996 *J. Phys. A: Math. Gen.* **29** 3707
[19] Thylwe K-E 2004 *J. Phys. A: Math. Gen.* **37** L589
[20] Yanoa T, Ezawab Y, Wadac T and Ezawad H 2003 *J. Comput. Appl. Math.* **152** 597
[21] Matzkin A, Jungen Ch and Ross S C 1998 *Phys. Rev.* A **58** 4462
[22] Andersson N 1993 *J. Phys. A: Math. Gen.* **26** 5085
[23] Sidky E Y and Ben-Itzhak I 1999 *Phys. Rev.* A **60** 3586
[24] Korsch H J, Laurent H and Möhlenkamp R 1982 *J. Phys. B: At. Mol. Phys.* **15** 1
[25] Fröman P O, Larsson K and Hökback A 1999 *J. Math. Phys.* **40** 1764
[26] Fröman N and Fröman P O 1993 Phase-integral method: the phase integral obtained numerically *Proc. 4th Int. Colloquium on Differential Equations (Plovdiv)* vol 1 ed D Bainov, V Covachev and A Dishliev pp 61–72
[27] Eckart C 1930 *Phys. Rev.* **35** 1303
[28] Epstein P S 1930 *Proc. Natl Acad. Sci. USA* **16** 627
[29] Karlsson F 1975 *Phys. Rev.* D **11** 2120
[30] Matzkin A 2000 *Phys. Rev.* A **63** 012103
Matzkin A 2001 *J. Phys. A: Math. Gen.* **34** 5085